Revisiting Lucas-Kanade and Horn-Schunck

Article · April 2013

DOI: 10.5963/JCEI0102001

CITATIONS
5

READS
1,680

4 authors:

Andry Maykol Pinto
Institute for Systems and Computer Engineering, Technology and Science (INESC …
34 PUBLICATIONS **195** CITATIONS
SEE PROFILE

A. Paulo Moreira
University of Porto
221 PUBLICATIONS **1,568** CITATIONS
SEE PROFILE

Paulo José Cerqueira Gomes da Costa
University of Porto
152 PUBLICATIONS **647** CITATIONS
SEE PROFILE

Miguel Velhote Correia
University of Porto
169 PUBLICATIONS **590** CITATIONS
SEE PROFILE

Revisiting Lucas-Kanade and Horn-Schunck

Andry Maykol G. Pinto[*1], A. Paulo Moreira[2], Paulo G. Costa[3], Miguel V. Correia[4]

INESC TEC and Department of Electrical and Computer Engineering,
Faculty of Engineering of the University of Porto, Rua Dr. Roberto Frias, Portugal
[*1]andry.pinto@fe.up.pt; [2]amoreira@fe.up.pt; [3]paco@fe.up.pt [4]mcorreia@fe.up.pt

***Abstract*-This paper revisits classical Lucas-Kanade (LK) and Horn-Schunck (HS) optical flow techniques. The aim is to provide a baseline for other researchers on these two timeless techniques. The formulations presented incorporate modern practices, namely multichannel, multi-resolution with refinement procedure (warping), non-quadratic penalisers and non-linear formulation of the brightness assumption. The experiments conducted demonstrate the performance enhancement that can be assigned to each modern practice. Thereby, the performance of the LK and HS is renewed in order to enable a fair comparison to other state-of-art techniques.**

Keywords- Optical Flow; Lucas-Kanade; Horn-Schunck; Colour; Multi-Resolution

I. INTRODUCTION

The good performance of today's optical flow formulations is possible due to several modern practices, namely multi-resolution (coarse-to-fine) refinement that deals with large displacements, iterative methods based on warping interpolations, multi-channels, robustification of each channel (non- quadratic penalisers), gradient constancy assumption to handle small variation of the brightness value, and photometric colour spaces. Usually, the performance of state-of-art techniques is compared to the classical Lucas-Kanade (LK) and Horn-Schunck (HS) presented by *Barron et al. (1994)* [2]. We consider these comparisons unfair because the LK and HS do not contemplate the most important modern practices (such as, multi-resolution with refinement, nonlinear formulation of the brightness constancy assumption). Therefore, the full potential of both techniques is not considered. For that reason, this article intends to provide a modern formulation of the LK and HS that incorporates multi-channel, multi-resolution with refinement (iterative procedure based on warping) and nonlinear brightness assumption. In addition, non-quadratic penaliser based on the *Charbonnier* error function is considered for the neighbourhood weighting of the LK.

Thereby, the contributions of this paper include:

- Modern and coloured formulation of the LK and HS
- Extensive qualitative and quantitative evaluation
- Baseline performance analysis for other research

The experimental analysis includes comparisons of both non-hierarchical and hierarchical pyramidal architectures. The contribution of the iterative refinement and multi-channel approach is also studied. Finally, the neighbourhood weights of the LK are iteratively defined using the non-quadratic penaliser. When implemented with appropriate and modern practices, classical optical flow formulations such as Lucas- Kanade [9] and Horn-Schunck [10] can achieve respectable optical flow estimations.

The article is organised as follows. Section II presents the major concepts beyond the optical flow formulation. Section III and Section IV present the multi-channel and multi-resolution LK and HS formulations, respectively. Section VI presents a comparative study between several versions of LK and HS. Finally, Section VII presents the most important conclusions.

II. CONCEPTS OF THE OPTICAL FLOW

Differential methods use several assumptions, such as brightness constancy and temporal consistence. These assumptions lead to a well-known motion constraint (approximated by the first order of Taylor's expansion).

$$\nabla I^T . \boldsymbol{v} + I_t = 0 \tag{1}$$

where $\boldsymbol{v} = (u, v)^T$ is the optical flow (horizontal and vertical velocities), $\nabla \mathbf{I} = (\mathbf{I_X}, \mathbf{I_Y})^{\mathrm{T}}$ is the spatial intensity gradient and $\mathbf{It}$ denotes the temporal derivative at time t. The motion constraint is an ill-state problem because there is one equation for two unknowns. Therefore, the measurements are under-constrained and a unique solution cannot be obtained for each position. This inability to measure the motion is known as the *aperture problem*. In some situations, it is only possible to infer about the velocity component in the same direction of the spatial gradient. Therefore, additional constraints are required in order to obtain a well-stated problem. There are several techniques that resort to different assumptions, namely, the neighbour concept that is used to estimate the optical flow. For many years, differential optical flow techniques were classified as local [9] and global [10]. More recent approaches combine both concepts using energy functionals [6], [12].

DOI: 10.5963/JCEI0102001

Coloured versions of LK and HS are reformulated in this article, see Sections III and IV. Furthermore, a coloured image $\mathbf{I}(\mathbf{x}) = (\mathbf{I}_1(\mathbf{x}), \mathbf{I}_2(\mathbf{x}), \mathbf{I}_3(\mathbf{x}))$ is represented by their channels, where $\mathbf{I_i}(\mathbf{x})$ denotes a single channel and $\mathbf{x} = (\mathrm{x}, \mathrm{y}, \mathbf{t})$.

III. COLOUR VERSION OF THE LUCAS-KANADE

The *Spatial coherence* assumption is generally used by local techniques. This assumption means that neighbour pixels move coherently and share the same flow. For instance, surrounding pixels belonging to the same surface are likely to move together [4], [3]. These neighbours introduce additional constraints, thus making the problem well-stated and over constrained.

By combining several motion constraints using local neighbours for each position, the optical flow can be estimated by minimising the sum of constraints over the neighbourhood of size σ and, as a result, the system can be solved for each pixel position, **x,** using a standard least-squares regression. The most used local technique, the Lucas-Kanade method [9], focuses on this principle; however, it was originally presented for brightness information. The local method used by this research is an extended and multichannel version of LK. It combines the three channels and consequently increases the gradient information that is used for the estimation. Thus, minimising the error in respect to the unknown optical flow variables, u and v:

$$min_{u,v} E_{LK} = \sum_{i=1}^{3} G_\sigma * \left[I_{ix}(\boldsymbol{x}).u + I_{iy}(\boldsymbol{x}).v + I_{it}(\boldsymbol{x})\right]^2 \quad (2)$$

where G_σ denotes a Gaussian convolution kernel with deviation σ, which controls the contribution of the neighbours and defines the main contribution for the least-square computation. I_{ix}, I_{iy} and I_{it} are spatial and temporal derivatives for a single channel, i ϵ {1, 2, 3}. Applying the weighted least-squares to Equation 2:

$$\begin{bmatrix} \sum_{i=1}^{3} G_{i\sigma} {I_{ix}}^2 & \sum_{i=1}^{3} G_{i\sigma} I_{ix} I_{iy} \\ \sum_{i=1}^{3} G_{i\sigma} I_{ix} I_{iy} & \sum_{i=1}^{3} G_{i\sigma} {I_{iy}}^2 \end{bmatrix} \begin{bmatrix} u \\ v \end{bmatrix} = - \begin{bmatrix} \sum_{i=1}^{3} G_{i\sigma} I_{ix} I_{it} \\ \sum_{i=1}^{3} G_{i\sigma} I_{iy} I_{it} \end{bmatrix} \quad (3)$$

The solution exists when the system matrix is invertible. This happens when it has rank 2 since both eigenvalues are not zero and the system can be solved using Cramer's rule. The size of the neighbourhood, σ, is the major concern of this technique because it cannot be enough to estimate the flow. Textureless image regions make the system matrix singular and a confidence measurement can be obtained based on the smallest eigenvalue [2].

IV. COLOUR VERSION OF THE HORN-SCHUNCK

Unlike local methods, global approaches use a smoothness term to avoid singularities. This smoothness term allows the neighbourhood information to be propagated across uniform regions.

The best known global technique is the Horn-Schunck [10] and it focuses on the minimisation of a quadratic error. The method has two terms, namely, the data-term that penalises the deviation from the motion constraint (Equation 1) and a smoothness term, also known as regularity term that penalises the deviation from the *smoothness flow* assumption. Recasting the HS, their data term is extended to a multichannel formulation by coupling all the channels [12]. A coloured version of the HS method can be reformulated as:

$$min_{\boldsymbol{v}} E_{HS} = \int_I \left[\sum_{i=1}^{3} \nabla I_i(x).\boldsymbol{v} + \lambda |\nabla \boldsymbol{v}|^2\right] d\mathrm{x}\mathrm{d}\mathrm{y} \quad (4)$$

where λ is the regularisation constant and $|\nabla \boldsymbol{v}| = |\nabla u|^2 + |\nabla v|^2$. This functional can be minimised by using the Euler-Lagrange equations with Neumann boundary conditions.

$$\hat{I}_x{}^2 u + \hat{I}_x \hat{I}_y v + \hat{I}_x \hat{I}_t - \lambda \Delta u = 0 \quad (5)$$

$$\hat{I}_x \hat{I}_y u + \hat{I}_y{}^2 v + \hat{I}_y \hat{I}_t - \lambda \Delta v = 0 \quad (6)$$

where Δ denotes the spatial Laplace operator that is numerically approximated by finite differences (a rectangular spacing grid $\mathrm{h_x}$ and $\mathrm{h_y}$ is used for x and y- directions) and the derivative according to j ϵ {x, y, t} is represented by $\hat{\mathbf{I}}_\mathbf{j} = \mathbf{I_{1j}} + \mathbf{I_{2j}} + \mathbf{I_{3j}}$. The filling-in effect is the major advantage of the HS because it allows the flow to propagate in locations that do not exhibit sufficient gradient information ($|\nabla \boldsymbol{I}| = 0$) [7]; however, the average caused by the smoothness-term blurs the flow at the motion boundary [3].

V. MODERN FORMULATIONS

First-order approximation of Taylor's expansion induces a linearisation of the motion constraint that is only valid for small optical flow values. Also, large optical flow displacements cause aliasing and multimodal energy functionals that may stop the minimisation process at local minimums [5].

Thus, the optical flow constraint is changed to a nonlinear formulation, $\boldsymbol{I}(\mathbf{x} + \mathbf{w}) - \boldsymbol{I}(\mathbf{x}) = 0$, yielding the Equations 7 and 8. A pyramidal structure of downsampled images can deal with large displacements. At each level, the current flow is used to warp the image at time $(\mathbf{t} + 1)$ towards the image at time $\mathbf{t}$ [3], [7]. The motion flow increments are obtained by

DOI: 10.5963/JCEI0102001

minimising the following energy functionals.

$$min_{\delta \boldsymbol{w}_l} \mathrm{E_{LK}} = G_\sigma * [I(\boldsymbol{x}+\boldsymbol{w_l}) - I(\boldsymbol{x})]^2 \quad (7)$$

$$min_{\delta \boldsymbol{w}_l} \mathrm{E_{HS}} = \int_I [I(\boldsymbol{x}+\boldsymbol{w_l}) - I(\boldsymbol{x})]^2 + \lambda |\nabla(\boldsymbol{w}_l + \delta \boldsymbol{w}_l)|^2 dxdy \quad (8)$$

where $\mathbf{w_l} = (u_l, v_l, 1)^T$ denotes the flow estimation and $\delta \mathbf{w}_l$ is the flow increment at pyramid level $l \in \{0, 1, ...\}$. The minimisation of the energy functionals, Equations 7 and 8, is conducted with regard to $\delta \mathbf{w}_l$.

A low-pass Gaussian filter with standard deviation $\sqrt{2/4\tau}$ [12] is applied prior to downsampling the input images by a factor of $\tau \in (0, 1)$. After that, a bicubic interpolation and the flow estimation from the coarser level are used to warp the image.

The temporal derivative is approximated by the first order of Taylor expansion, Equation 9, in order to remove the non-linearity from the equations above.

$$I_t = I(\boldsymbol{x}+\boldsymbol{w}) - I(\boldsymbol{x}) \quad (9)$$

Therefore,

$$I_{t,l+1} \cong I(\boldsymbol{x}+\boldsymbol{w_l}) - I(\boldsymbol{x}) + I_{x,l}\delta u_l + I_{y,l}\delta v_l$$

$$\therefore\ I_{t,l+1} = I_{x,l}\delta u_l + I_{y,l}\delta v_l + I_{t,l} \quad (10)$$

where $\mathbf{I_{X},}_l$ and $\mathbf{I_{Y},}_l$ are the spatial derivatives of $\mathbf{I}(\mathbf{x}+\mathbf{w}_l)$. This linearisation enables a proper minimisation of Equations 7 and 8.

Therefore, minimising Equation 7 is a straightforward process, while Equation 8 yields the Euler- Lagrange equations:

$$\hat{I}_{x,l}\left[\hat{I}_{x,l}\delta u_l + \hat{I}_{y,l}\delta v_l + \hat{I}_{t,l}\right] - \lambda \Delta u_{l+1} = 0 \quad (11)$$

$$\hat{I}_{y,l}\left[\hat{I}_{x,l}\delta u_l + \hat{I}_{y,l}\delta v_l + \hat{I}_{t,l}\right] - \lambda \Delta v_{l+1} = 0 \quad (12)$$

where $u_{l+1}=u_l + \delta u_l$ and $v_{l+1} = v_l + \delta v_l$. The optical flow is divided into two variables, namely, the flow of the coarser level and the unknown flow increment of the current pyramid level. At each level, the flow increment is small due to a multi-resolution approach and, therefore, the linearisation is valid.

The optical flow estimation begins at the coarsest level and refines the solution by considering the current flow estimation to warp the input image before the next finer level. Thus, $\delta \mathbf{w}_l$ is obtained between the partially registered images. Finally, the current flow estimation, $\mathbf{w}_l$, is updated at the end of each level. The minimisation scheme used in this article follows the classical HS [10]; however other minimisation schemes can be used, for instance, successively over relaxation. To discretise the Euler-Lagrange equations, the temporal derivative is approximated by a two-point stencil [−1, 1], the spatial flow derivatives are approximated by a second order stencil [−1, 0, 1] /2h and spatial image derivatives are approximated via a central finite difference by a fourth order approximation and using the stencil [1, −8, 0, 8, −1] /12h, where h is the grid size.

For the LK method, Equation 7, instead of using a Gaussian convolution to define the contribution of each neighbour according to their distance to the current estimation position, it is possible to set the weights using a non-quadratic penaliser. This identifies the neighbours that violate the coherence assumption. This way, neighbours that do not have the same motion will have a lower weight and, therefore, their importance for the estimation is reduced. This increases the accuracy of the estimation (see the experiments section). This paper considers the *Charbonnier* error function.

VI. EXPERIMENTS

The methods are implemented using similar schemes to enable a more reliable comparison between them. They are tested under test sequences [1] and considering the average angular error (AAE) [2] and average end-point error measurements (EPE) [1]. The modern implementations of the HS and LK use a median filter in current flow estimate and between the intermediate stages of the incremental optimisation architecture to increase the performance of the estimation.

A bicubic interpolation is used by the warping process and the scaling parameter of the *Charbonnier* penaliser is set to 0.001. A Gaussian convolution smoothing filter is applied to the image sequence in order to reduce the noise and to make the image infinitely many times differentiable [12].

The following optical flow versions are evaluated:

- Single-colour LK: original [9], multi-resolution (MR) and a multi-resolution with iterative refinement (MR+IR),

DOI: 10.5963/JCEI0102001

similar to the formulation presented in Equation 7, but considering one channel - brightness;

- Multi-colour LK: multi-resolution with iterative refinement (MR+IR), formulation presented in Equation 7, and the MR+IR with weights obtained by a non- quadratic penaliser;
- Single-colour HS: original [10], multi-resolution (MR) and a multi-resolution with iterative refinement (MR+IR), similar to the formulation presented in Equation 8, but for a single channel - brightness;
- Multi-colour HS: multi-resolution with the iterative refinement (MR+IR), formulation presented in Equation 8.

Thus, this paper studies the impact of several modern practices in the performance of the classical HS and LK formulation, namely the pyramidal structure, the iterative refinement and the multi-colour space. All the reported experiments have been conducted considering 100% density.

A. LK Modern Formulation

TABLE I COMPARISON BETWEEN THE ORIGINAL LUKAS-KANADE [9], A MULTI-RESOLUTION (MR) AND A MULTI-RESOLUTION WITH ITERATIVE REFINEMENT VERSION (MR+IR). THE PERFORMANCE RESULTS OF THESE VERSIONS ARE REPORTED USING THE AVERAGE ANGULAR (◦) AND THE STANDARD DEVIATION (IN PARENTHESES)

Sequence	Original	MR	MR+IR
Dimetrodon [1]:	21.23 (21.26)	12.66 (19.05)	12.39 (18.73)
Grove2 [1]:	28.84 (21.20)	4.95 (9.80)	4.81 (9.58)
Grove3 [1]:	32.74 (31.50)	9.27 (17.98)	9.06 (18.21)
RubberWhale [1]:	18.52 (21.74)	14.23 (21.54)	14.15 (21.66)
Hydragea [1]:	27.87 (24.81)	9.27 (18.90)	9.11 (19.56)
Urban2 [1]:	45.47 (41.04)	9.19 (18.03)	9.04 (20.14)
Urban3 [1]:	48.14 (43.20)	7.74 (20.36)	7.00 (18.84)

Table I presents the experiments conducted for several LK versions. The aim is to demonstrate the improvement gain that can be accomplished by an optical flow technique that resorts to a hierarchical structure with iterative refinement.

As expected, a pyramidal structure substantially increases the performance of the estimation. It makes it possible to estimate large motion displacements and this factor reflects the overall performance. The iterative refinement procedure makes it possible to incorporate the non-linear motion constraint into the formulation of the method. The accuracy of the flow estimation is also increased, since small motion increments are successively estimated throughout the minimisation process.

For single-channel formulations, the hierarchical structure with the iterative refinement method (MR+IR) has proved to be the technique with the best results for all the sequences, see Table I. It was demonstrated that modern practices significantly enhance the performance of the optical flow methods, even the more classical formulations like Lucas- Kanade and Horn-Schunck.

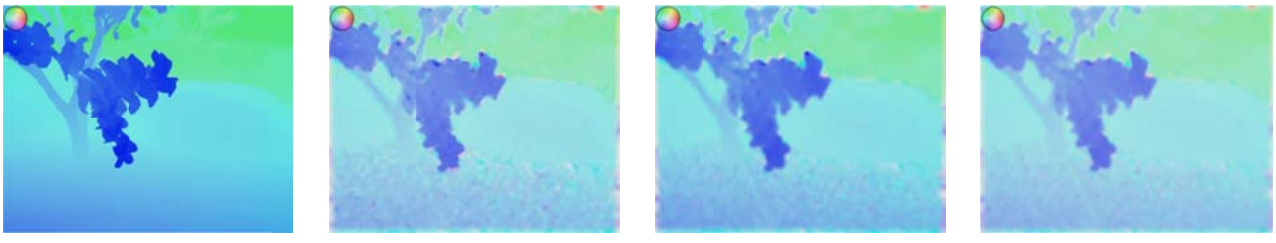

(a) GT (b) MR+IR (c) Colour + MR+IR (d) Robust + Color + MR+IR

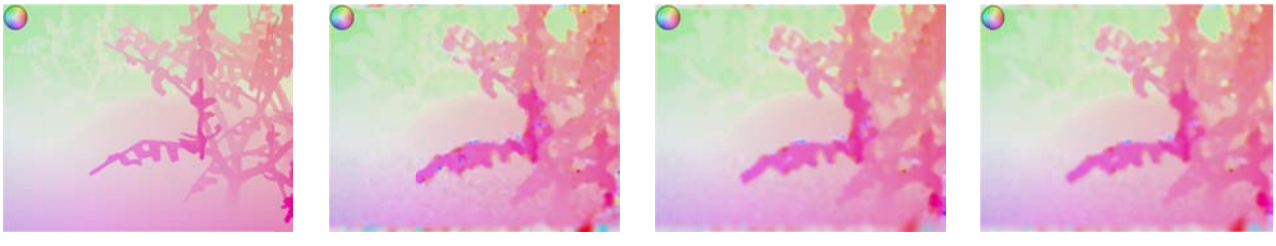

(e) GT (f) MR+IR (g) Color + MR+IR (h) Robust + Color + MR+IR

DOI: 10.5963/JCEI0102001

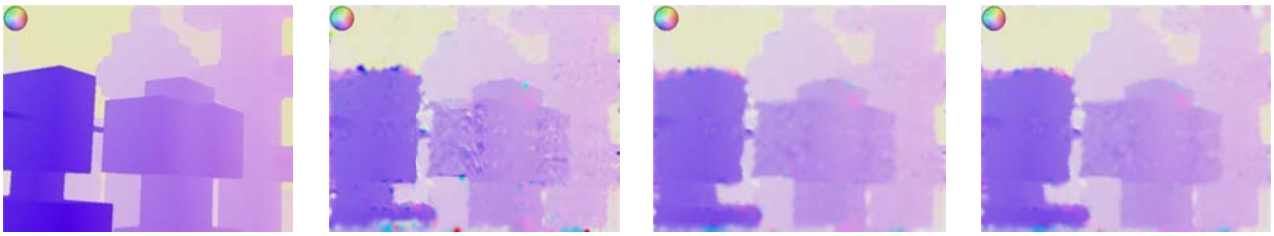

(i) GT (j) MR+IR (k) Colour + MR+IR (l) Robust + Colour + MR+IR

Fig. 1 Multi-resolution with refinement LK formulation, under Middleburry test sequences. The first column is the ground truth, the second is the single channel LK, the third is the multi-channel LK and the fourth is the multi-channel with the weighting function obtained by a non-quadratic penaliser. The images are represented using HSV colour space, where the hue-channel measures the direction of the flow vector and the saturation measures the magnitude of the optical flow. From top to bottom, the sequences are: Grove2, Grove3 and Urban3

TABLE II RESULT OF THE MULTI-CHANNEL AND MULTI-RESOLUTION WITH ITERATIVE REFINEMENT (MR+IR) LK VERSION AND RESULTS OF THE MULTI-CHANNEL AND MULTI-RESOLUTION WITH ITERATIVE REFINEMENT LK VERSION WHERE THE NEIGHBOURHOOD WEIGHTS ARE OBTAINED BY A NON-QUADRATIC ERROR FUNCTION (ROBUST+MR+IR). THE PERFORMANCE RESULTS OF THESE VERSIONS ARE REPORTED USING THE AVERAGE ANGULAR ERROR (AAE) AND THE AVERAGE END-POINT ERROR (EPE)

Sequence	MR+IR		Robust+MR+IR	
	AAE	EPE	AAE	EPE
Dimetrodon [1]:	8.48 (14.95)	0.392	7.49 (13.84)	0.344
Grove2 [1]:	4.08 (8.26)	0.308	3.78 (7.67)	0.275
Grove3 [1]:	8.18 (16.39)	0.988	7.69 (15.95)	0.919
RubberWhale [1]:	9.68 (18.74)	0.345	9.05 (18.74)	0.318
Hydragea [1]:	6.87 (18.46)	0.468	6.54 (17.99)	0.426
Urban2 [1]:	7.78 (17.39)	0.572	7.04 (15.77)	0.431
Urban3 [1]:	5.53 (16.64)	0.862	5.25 (16.11)	0.825

Table II depicts the improvement resulting from the colour information. In this table, the performance of a multi-channel with MR+IR version is compared to a more robust version where the weights are defined by a non-quadratic penaliser. As can be seen, the multi-channel technique performs better than a single-channel version. Figures 1(b), 1(f) and 1(j) present some results for the single-channel MR+IR LK version, and figures 1(c), 1(g) and 1(k) present results of the multi-channel LK version. Finally, the last LK technique uses multi-colour with "robustification", which makes it possible to identify the neighbours that do not have similar motion, for instance, it detects the neighbours that violate the coherence assumption by reducing their associate weight.

This is an important assumption to formulate the LK method and the quality of the flow is measured for each neighbour using the linear motion constraint. Figures 1(d), 1(h) and 1(l) depict the results of a multi-channel MR+IR LK version with robustification.

As it is possible to confirm, the robustification increases the performance of the optical flow estimation. Multi-channel approaches use more information to estimate the optical flow. Therefore, a multi-channel formulation that combines a hierarchical estimation, iterative refinement and a measurement of the coherence assumption achieves a respectable performance.

TABLE III COMPARISON BETWEEN THE ORIGINAL HORN-SCHUNCK[10], A MULTI-RESOLUTION (MR) AND A MULTI-RESOLUTION WITH ITERATIVE REFINEMENT VERSION (MR+IR). THE PERFORMANCE RESULTS OF THESE VERSIONS ARE REPORTED USING THE AVERAGE ANGULAR ERROR (°) AND THE STANDARD DEVIATION (IN PARENTHESES)

Sequence	Original	MR
Dimetrodon [1]:	38.13 (20.30)	13.59 (17.33)
Grove2 [1]:	25.77 (20.66)	7.68 (10.11)
Grove3 [1]:	30.78 (30.00)	18.25 (27.33)
RubberWhale [1]:	22.36 (20.47)	14.37 (20.09)
Hydragea [1]:	31.10 (24.65)	12.17 (21.14)
Urban2 [1]:	43.34 (37.29)	17.89 (26.25)
Urban3 [1]:	51.51 (34.81)	15.71 (24.78)

DOI: 10.5963/JCEI0102001

TABLE IV RESULTS OF THE SINGLE-CHANNEL AND MULTI-RESOLUTION WITH ITERATIVE REFINEMENT (MR+IR) HS VERSION AND RESULTS OF THE MULTI-CHANNEL AND MULTI-RESOLUTION WITH ITERATIVE REFINEMENT (MR+IR+COLOUR) HS. THE PERFORMANCE RESULTS OF THESE VERSIONS ARE REPORTED USING THE AVERAGE ANGULAR ERROR (AAE) AND THE AVERAGE END-POINT ERROR (EPE)

Sequence	MR+IR		MR+IR+Colour	
	AAE	EPE	AAE	EPE
Dimetrodon [1]:	13.67 (18.76)	0.595	10.02 (17.03)	0.454
Grove2 [1]:	4.10 (7.75)	0.307	3.90 (7.96)	0.290
Grove3 [1]:	7.82 (15.38)	0.920	7.29 (14.91)	0.854
RubberWhale [1]:	14.27 (20.98)	0.492	10.70 (20.08)	0.432
Hydragea [1]:	8.74 (18.52)	0.468	6.72 (14.09)	0.495
Urban2 [1]:	6.72 (14.09)	0.398	5.57 (15.93)	0.330
Urban3 [1]:	13.57 (24.41)	0.910	12.98 (27.58)	0.800

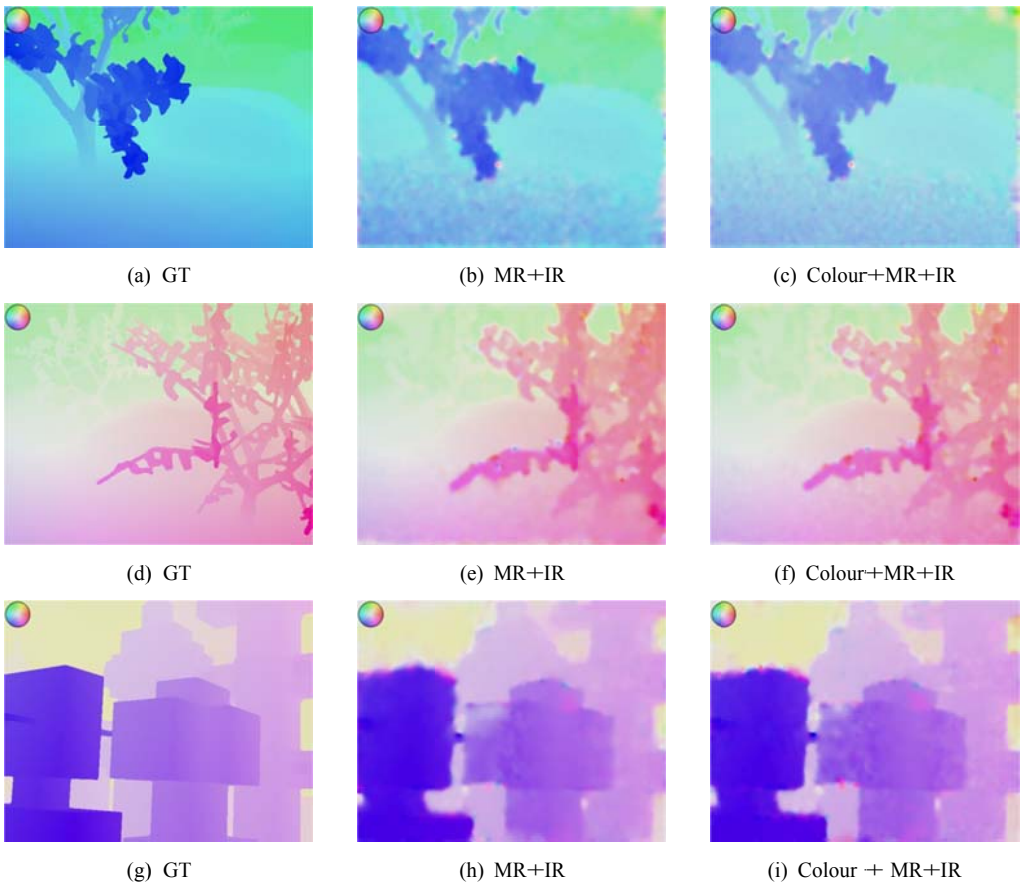

(a) GT (b) MR+IR (c) Colour+MR+IR

(d) GT (e) MR+IR (f) Colour+MR+IR

(g) GT (h) MR+IR (i) Colour + MR+IR

Fig. 2 Multi-resolution with refinement HS formulation, under Middleburry test sequences. The first column is the ground truth, the second is the single channel HS and the third is the multi-channel HS. The images are represented using HSV colour space, where the hue-channel measures the direction of the flow vector and the saturation measures the magnitude of the optical flow. From top to bottom, the sequences are: Grove2, Grove3 and Urban3

B. HS Modern Formulation

The performance of four HS versions are analysed during this section, namely, the original formulation [10], multi-resolution, multi-resolution with iterative refinement, and multi-resolution and multi-colour with iterative refinement.

Table III presents the performance improvement due to the pyramidal-based HS formulation. A pyramidal formulation is, perhaps, the most important modern practice since the performance gain is very significant.

Table IV compares the performance of a single and multi-colour MR+IR HS techniques. Figures 2(b), 2(e) and 2(h) present some results for the single-channel MR+IR HS version, and Figures 2(c), 2(f) and 2(i) presents results of the multi-channel HS version.

The HS versions present results which are similar to the ones presented by the LK. The MR+IR formulation has a strong impact on the overall performance of the technique. The performance gain achieved due to colour information seems to be lower than that achieved with the LK versions; however, colour plays an important role in estimating optical flow, see Table IV.

DOI: 10.5963/JCEI0102001

During the experiments conducted, the LK version performs generally better than the coloured version of HS, compare Figures 1(d), 1(h) and 1(l) with Figures 2(c), 2(f) and 2(i). However, in most cases the difference between both performances is too small.

Finally, the median filter has a major impact on the optical flow estimation. All the results reported during this article were obtained by considering a median filter. This median filter was applied at the end of each intermediate stage of the MR and MR+IR process. The improvement achieved by the median filter is very large and, therefore, their use is highly recommended (instead, a bilateral filter can also be considered).

VII. CONCLUSION

The Lucas-Kanade and Horn-Schunck optical flow methods are revisited in this article. Modern practices are applied to each classical formulation, namely, hierarchical multi-resolution architecture, iterative refinement and multi-channel. These modern practices intend to renew each method in order keep their performance updated. The aim is to enable a more reasonable and fair comparison to other state-of-art techniques.

The non-linear motion constraint is considered in both formulations. The minimisation is conducted using the iterative refinement procedure in a multi-resolution structure, allowing small incremental motions to be estimated, which reflects a more accurate optical flow. Perhaps, the most important modern practice is the multi-resolution strategy because it can deal with large motion displacements. The results demonstrate their importance since the estimation performance was substantially improved.

The multi-channel approach is also a significant advantage to estimate the optical flow. In addition, a robust penaliser based on *Charbonnier* error function was also integrated into a multi-resolution with iterative refinement and multi-channel LK formulation. The experiments proved that this LK version leads to a better performance comparatively to other versions. This result is expected since the non-quadratic penaliser turns the spatial coherence assumption more robust than neighbours that violate the assumption.

Modern practices enhance the performance of classical HS and LK formulations, making them competitive comparatively to more modern optical flow techniques. Therefore, results of this article renew the performance of these two timeless optical flow techniques.

ACKNOWLEDGMENT

This work is funded by the Portuguese Government through the FCT - Foundation for Science and Technology, SFRH-BD-70752-2010.

REFERENCES

[1] Baker, Simon, Scharstein, Daniel, Lewis, J., Roth, Stefan, Black, Michael, Szeliski, Richard. “A Database and Evaluation Methodology for Optical Flow”. International Journal of Computer Vision, 92(1), 1-31, 2011.

[2] Barron, J., Fleet, D., Beauchemin, S. “Performance of optical flow techniques”. International Journal of Computer Vision, 12(1), 43-77, 1994.

[3] Black, Michael Julian. “Robust Incremental Optical Flow”. PhD thesis in computer science, Yale University, Department of Computer Science, Yale, 1992.

[4] Bradski, Gary, Kaehler, Adrian. “Learning OpenCV: Computer Vision with the OpenCV Library”. O Reilly Media Inc., first edition, 2008.

[5] Brox, T., Bruhn, A., Papenberg, N., Weickert, J. “High accuracy optical flow estimation based on a theory for warping”. European Conference on Computer Vision (ECCV), 4, 2536, 2004.

[6] Bruhn, A., Weickert, J., Schnorr, C. “Lucas/Kanade meets Horn/Schunck: Combining local and global optic flow methods”. International Journal of Computer Vision, 61(3), 211-231, 2005.

[7] Fleet, David J. and Weiss, Yair. “Mathematical models for Computer Vision: The Handbook”. N. Paragios, Y. Chen, and O. Faugeras (eds.), Springer, first edition, 2005.

[8] Fleet, D. and Jepson, A. “Computation of component image velocity from local phase information”. International Journal of Computer Vision, 5(1), 77-104, 1990.

[9] Lucas, Bruce D., Kanade, Takeo. “An Iterative Image Registration Technique with an Application to Stereo Vision”. In International Joint Conference on Artificial Intelligence (IJCAI), 674679, 1981.

[10] Horn, Berthold K.P., Schunck, Brian G. “Determining optical fow Artificial Intelligence”, 17(1), 185203, 1981.

[11] Sun, D., Roth, S., Black, M. “Secrets of optical flow estimation and their principles”. IEEE Conference on Computer Vision and Pattern Recognition, 2432-2439, 2010.

[12] Zimmer, Henning and Bruhn, Andrés and Weickert, Joachim. “Optical Flow in Harmony”. International Journal of Computer Vision, 93(3), 368-388, 2011.

DOI: 10.5963/JCEI0102001